Tailoring the Chemical Structure of Nitrogen-Doped Carbon Dots for Nano-Aminocatalysis in Aqueous Media

Giuseppe Gentile,[a] Martina Mamone,[a] Cristian Rosso,[a, b] Francesco Amato,[a, c] Chiara Lanfrit,[a] Giacomo Filippini,*[a] and Maurizio Prato*[a, d, e]

Amine-rich carbon dots (NCDs) have become promising nano-aminocatalytic platforms in organic synthesis. These nano-materials can be effectively produced through straightforward bottom-up approaches using inexpensive nitrogen-containing molecular precursors as a starting material. However, to date, there is still a limited understanding of how the molecular features of these precursors affect the catalytic activity of the resulting nanoparticles. This study concerns the production of a new family of NCDs, which use L-arginine and different alkyl diamines as starting materials. The surface amines of all these NCDs were comprehensively characterized, thus allowing us to provide a correlation between the structural features of the nanoparticles and their catalytic performance with a selected amino-catalyzed organic transformation. Importantly, the most active nano-aminocatalysts, namely, NCDs-**3**, were then used as a basis for the formation of a wide variety of functionalized organic compounds in water under mild reaction conditions.

Introduction

Carbon dots (CDs) are an emerging class of quasi-spherical carbon-based nanoparticles with dimensions below 10 nm.[1–4] In recent years, these nanomaterials have gained popularity thanks to their excellent luminescence and optical features, considerable solubility in aqueous and polar solvents, high chemical and photostability, as well as their low toxicity and excellent biocompatibility.[3,5,6] Moreover, CDs can be readily produced from inexpensive and abundant molecular precursors through straight-forward and robust bottom-up synthetic protocols.[7,8] Interestingly, when molecules are used as precursors, the structure of the

resulting CDs may reflect the molecular features of the starting materials.[1,9,10] Thus, the appropriate selection of the precursors and the operative conditions employed in the CD synthesis play a key role in defining the chemical nature and, in turn, the potential applications of the resultant nanomaterials.[11–14] From a structural point of view, CDs are typically core-shell nanoparticles consisting of carbon cores surrounded by shells bearing various polar groups, such as carboxylic acids, alcohols and amines.[15,16] In recent years, the presence of these reactive surface functionalities has allowed the exploitation of CDs in synthetic nano-organocatalysis for the production of valuable organic compounds under mild operative conditions.[13–15,17–19] In this context, nitrogen-doped amine-rich CDs (NCDs) are becoming extremely popular metal-free, nano-catalytic platforms due to their interesting properties.[2,20,21] Indeed, NCDs can be easily synthesized through the thermal treatment (i.e., carbonization, pyrolysis, or hydrothermal/microwave treatment) of suitable nitrogen-containing precursors such as amino acids, amines, and polyamines.[3] In this way, it is possible to produce nitrogen-doped particles that, through the amine moieties on their surfaces, can mimic the activation modes of classical molecular aminocatalysts at the nanoscale level.[22] Following this approach, Wang and co-workers recently reported a bottom-up method for the production of amine-terminated CDs (NCDs-**A**) using citric acid and different aliphatic amines as precursors (Figure 1a).[23]

Specifically, the authors demonstrated that the catalytic activity of NCDs-**A** towards Knoevenagel reactions may be modulated by selecting the substitution degree of the molecular amine used in the nanoparticles synthesis. In 2020, our group reported that NCDs-**2**, produced through the hydrothermal treatment of L-arginine (Arg) and 1,2-diaminoethane (EDA), can drive the functionalization of a variety of sterically hindered carbonyl compounds through enamine or iminium ion activations.[15] Interestingly, the formation of reactive iminium ion intermediates, on the surface of these nanoparticles, was observed by ^{19}F NMR spectroscopy using 4-fluorocinnamaldehyde as a molecular fluori-

[a] G. Gentile, M. Mamone, Dr. C. Rosso, Dr. F. Amato, C. Lanfrit, Dr. G. Filippini, Prof. M. Prato
Department of Chemical and Pharmaceutical Sciences, INSTM UdR Trieste
University of Trieste, via Licio Giorgieri 1, 34127 Trieste (Italy)
E-mail: gfilippini@units.it
prato@units.it

[b] Dr. C. Rosso
Present address: Department of Chemical Sciences
University of Padova, via Marzolo 1, 35131 Padova (Italy)

[c] Dr. F. Amato
Present address: Department of Chemistry
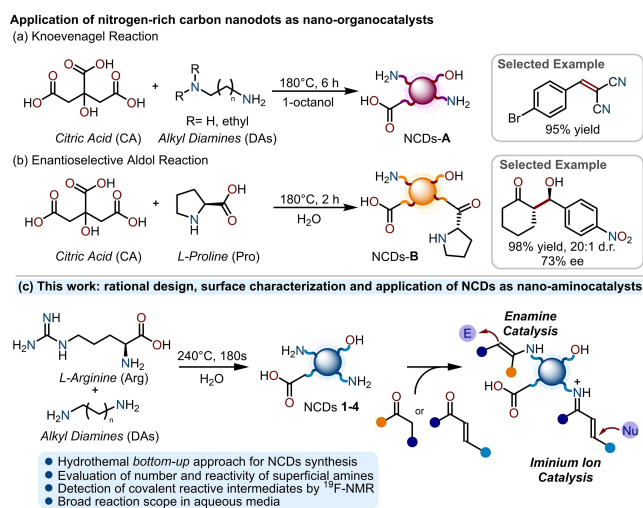University La Sapienza, p.le A. Moro 5, 00185 Roma (Italy)

[d] Prof. M. Prato
Center for Cooperative Research in Biomaterials (CIC BiomaGUNE)
Basque Research and Technology Alliance (BRTA)
Paseo de Miramón 194, 20014, Donostia San Sebastián (Spain)

[e] Prof. M. Prato
Basque Foundation for Science
Ikerbasque, 48013 Bilbao (Spain)

ChemSusChem

Research Article
doi.org/10.1002/cssc.202202399

Chemistry
**Europe**
European Chemical
Societies Publishing

Figure 1. (a) Use of NCDs-**A** for Knoevenagel reactions. (b) Enantioselective aldol reaction catalyzed by NCDs-**B**. (c) This work: use of structurally different NCDs **1–4** produced from L-arginine and alkyl diamines in nano-amino-catalysis.

nated probe. Recently, Xu and co-workers described the synthesis of novel chiral NCDs-**B** starting from citric acid and L-proline by hydrothermal treatment at 180 °C. These nanoparticles have been effectively used as catalysts to promote the direct catalytic asymmetric aldol reaction between cyclohexanone and 4-nitro-benzaldehyde (Figure 1b).[21] However, although these examples indicate that some of the chemical features of the molecular precursors are typically conveyed into the resulting nanomaterials, to date, chemists still have a limited understanding of this aspect and of how it may be exploited for a priori rational design of novel and more effective NCD-based catalysts. To address this issue, we prepared a library of amine-rich NCDs **1–4** using Arg as the main particle precursor along with different alkyl diamines (DAs) with progressively longer carbon skeletons (Figure 1c). These water-soluble nitrogen-doped nanoparticles were comprehensively characterized placing emphasis on the evaluation of the number, nature, and reactivity of the surface amino moieties. These insights enabled us to demonstrate a clear correlation between the structural features of the NCDs and their catalytic performance toward a selected amino-catalyzed organic transformation, namely, an aldol reaction between acetone (**1a**) and 4-nitro-benzaldehyde (**2a**). Subsequently, the most efficient catalytic carbon nanoparticles (NCDs-**3**) were used to catalyze many organic transformations in water under mild operative conditions. This is of practical importance since in recent year the use of water as a medium for organic reactions has attracted much interest.[24–28] Indeed, water offers many advantages because it is a cheap, readily available, non-toxic and non-flammable solvent, thus being very attractive from both an economical and an environmental point of view.[24]
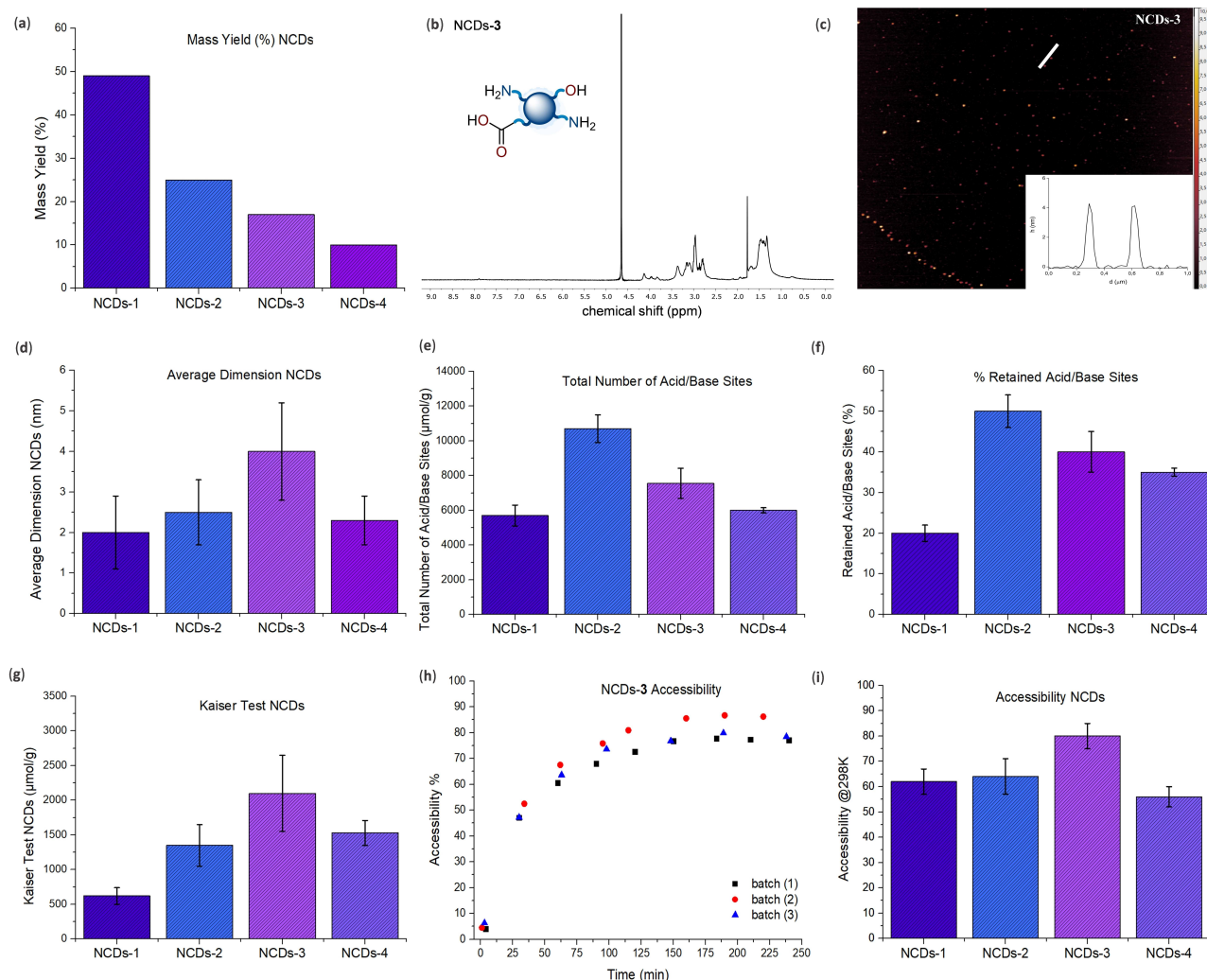
Results and Discussion

NCDs **1–4** were synthesized following a simple, fast, and robust microwave-assisted procedure (Figure 2),[8] which can be schematized as follows: (i) hydrothermal treatment of the molecular precursor(s) at 240 °C for 180 s; (ii) filtration of the crude reaction through a membrane (pore size of 0.1 μm) to remove large carbon particles and insoluble organic compounds; (iii) dialysis with water to remove soluble molecular species; and, finally, (iv) freeze-drying process to obtain the purified nanoparticles as yellowish solid materials (see Section B.1 of the Supporting Information for additional details). In particular, NCDs-**1** were obtained from Arg through a mono-component approach, while the utilization of different DAs – namely EDA, 1,4-diaminobutane (BDA) and 1,6-diaminohexane (HDA) – as nitrogen-doping agents, in combination with Arg (1:1 molar ratio), led to the production of NCDs **2–4**. Specifically, we assumed that the use of diverse molecular DAs as precursors could affect both the number and reactivity of the amino groups on the nanoparticle surfaces.

Indeed, ^{13}C NMR studies regarding the formation mechanism of this class of NCDs demonstrated that their aromatic cores mainly originate from Arg, while the diamine mostly contributes to the chemical structure of their external shells.[29,30] The mass yield of the purified NCDs (calculated as the percentage of the weight of the starting materials retained in the purified NCDs) shows that in the mono-component reaction (NCDs-**1**) roughly half of the amount of the starting material (Arg) is converted into the desired nanoparticles (Figure 3a). On the other hand, when Arg is used in combination with the alkyl diamines (NCDs **2–4**), the mass yield decreases progressively with the increase in the length of the carbon chain of the DA used. This decrease may be rationalized by considering that the responsiveness to microwave heating decreases as the reaction mixture becomes less polar, and therefore shows a lower dielectric constant.[31] This occurs when a DA bearing a long aliphatic carbon chain is employed in the synthesis, and thus a decreased efficiency in the heat transfer to the reaction mixture impedes the formation of the NCDs. Structural and morphological information on NCDs **1–4** was obtained by thermogravimetric analysis (TGA), attenuated total reflectance-Fourier-transform infrared spectroscopy (ATR-FTIR), NMR analysis, and atomic force microscopy (AFM, see Sections B.2.2. and B.2.3 of the Supporting Information for details). TGA confirmed the largely amorphous nature of NCDs **1–4**. In fact, around 90% of the total weight loss was observed at 600 °C under
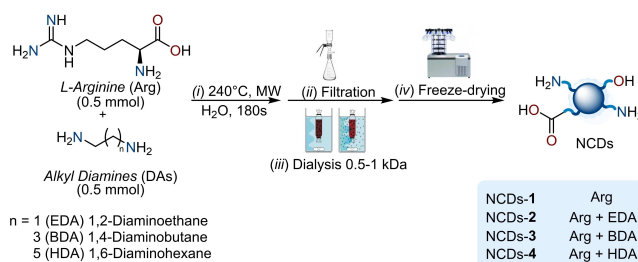
Figure 2. Synthesis and purification of NCDs **1–4** starting from L-arginine (Arg) and different alkyl diamines (DAs).

ChemSusChem

Research Article
doi.org/10.1002/cssc.202202399

**Chemistry
Europe**
European Chemical
Societies Publishing

Figure 3. (a) Mass yield histogram for NCDs **1–4**. (b) ^{1}H NMR (D$_2$O, 400 MHz) spectrum of NCDs-**3**. (c) Tapping mode AFM of NCDs-**3** deposited on a mica substrate; inset: height profile along the white solid line. (d) Size histogram of AFM height data. (e) Total number of acid/base sites obtained from back titration of NCDs **1–4**. (f) Retained percentage histogram of acid/base sites. (g) Kaiser test (KT) of NCDs **1–4** conducted at 393 K. (h) Plotting of accessibility curves for NCDs-**3** at 298 K. 100% of accessibility is set as KT value at 393 K. (i) Time dependent KT (accessibility) at 298 K for NCDs **1–4**.

nitrogen for NCDs **2–4**, while NCDs-**1** showed a slightly higher thermal stability. Focusing on the molecular structures of these nanoparticles, ATR-FTIR clearly points to the presence of N–H and O–H bonds, which provide solubility in water and polar solvents. Moreover, an intense band at 1540 cm^{-1} is compatible with the presence of primary amide bonds, which likely have a relevant role in the formation of NCDs **1–4**.[32] The presence of amide functionalities was further confirmed and quantified by bicinchoninic acid essay.[33] In this test, Cu^{II} is reduced selectively, in an alkaline buffer, to Cu^{I} by the amide bonds present in the nanoparticle.[34] Subsequently, Cu^{I} ions are chelated by two bicinchoninic acid moieties forming a tetrahedral complex with a characteristic absorption band at around 562 nm (see Supporting Information). ^{1}H NMR spectra of NCDs **1–4** (see Section B.2.2 of the Supporting Information and Figure 3b) display broad signals in the aliphatic (1–4 ppm) region of the spectrum. Importantly, the presence of broad signals is coherent with the formation of particles.[35] AFM analysis confirmed the nano-scale dimensions of

the NCDs **1–4**, that range from 2 to 4 nm (see Section B.2.2 of the Supporting Information and Figure 3c,d). The UV-Vis absorption spectra of NCDs **1–4** in water display broad absorption bands extending into the visible region up to 420 nm. In particular, non-structured shoulders appear at 225 nm and 290 nm, which can be attributed to the π–π* transition of conjugated C=C units (see Section B.2.1 of the Supporting Information).[36] Since none of the precursors absorbs more than 400 nm, the nanoparticle formation affords low-energy optical transitions in the visible region. NCDs **1–4** display a typical excitation wavelength-dependent fluorescence where the main emission band is centered at around 350 nm (see Supporting Information). Accordingly, quantum yield (QY) changes with the excitation wavelength. NCDs-**2**, for example, shows the highest QY value among the series, equal to 22.0%± 0.5% (excitation at 300 nm).
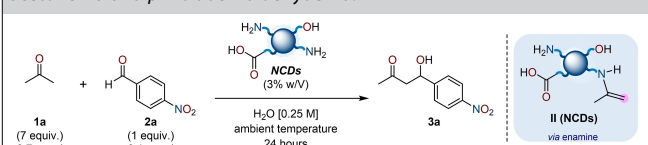
Subsequently, the intrinsic pH of the water-soluble nanoparticles was evaluated by dissolving NCDs **1–4** in milli-Q water (concentration of 2.5 mg mL^{-1}). All NCDs showed an alkaline

intrinsic pH ranging from 9 up to almost 10 (see Section B.2.3 of the Supporting Information). Specifically, we observed that the alkalinity increases from NCDs-**1** to NCDs-**4**. In addition, the quantification of the total number of acid/base sites was achieved by Gran Plot analysis, which consists of the linearization of a simple pH back titrations curve.[37] The analysis has shown that the number of acid/base sites ranges from a minimum of $5700 \pm 600 \, \mu mol \, g^{-1}$ for NCDs-**1** to a maximum of $10700 \pm 800 \, \mu mol \, g^{-1}$ for NCDs-**2** (Figure 3e). Moreover, if we compare the value of the acid/base sites in the initial mixture of precursors, it is possible to quantify retained sites on NCDs surfaces. In fact, some of the initial starting material acid/base moieties are lost during the synthesis due to decarboxylation reactions, dehydration, formation of amide bonds and appearance of molecular side-products that are removed from NCDs during the purification step.[5,38,39] Specifically, up to $50\% \pm 4\%$ of sites are retained for NCDs-**2** compared to just $20\% \pm 4\%$ for NCDs-**1**, showing a steep increase in the bi-component synthesis with respect to the mono-component approach (Figure 3f). Interestingly, a clear correlation can be observed between the total number of acid/base sites, the percentage of retained sites, and the length of the DA used (see Section B.2.3 of the Supporting Information). Indeed, besides the general increase of sites from mono- to bicomponent synthesis, the absolute number of sites retained and their percentage decrease consistently with the increase in the length of the diamine carbon chain (Figure 3f). Furthermore, agarose gel electrophoresis in a citrate buffer (pH 4) resulted in all NCDs **1**–**4** migrating toward the cathode in uniform blue emissive bands under UV-light irradiation (Figure S31). This indicates that NCDs **1**–**4** have a positive charge which could be consistent with the presence of protonated amino groups. Furthermore, the staining of the agarose gel with Coomassie brilliant blue dye highlighted the presence of positively charged nanoparticles by the appearance of blue spots, where the presence of NCDs was previously highlighted by fluorescence detection (Figure S32).[40] To further characterize the surface chemistry of NCDs, Kaiser Test (KT) was applied to detect and quantify the presence of superficial amines (Figure 3g).[41,42] In this analysis, ninhydrin reacts with aliphatic primary amines on the surface of nanomaterials to form Ruhemann's purple dye that can be detected and quantified by UV-vis spectroscopy. All NCDs tested positive for aliphatic primary amines with the rapid appearance of the characteristic purple color. Specifically, NCDs-**1** produced from Arg alone bear approximately $620 \pm 80 \, \mu mol \, g^{-1}$. On the other hand, when the DAs are used, the number of surface amines increases considerably. Interestingly, when the length of the diamine carbon chain is increased from 2 (NCDs-**2**) to 4 carbon atoms in NCDs-**3** the amines quantified by KT increased from $1350 \pm 300 \, \mu mol \, g^{-1}$ to $2100 \pm 550 \, \mu mol \, g^{-1}$. Unexpectedly, the number of amines does not increase in NCDs-**4** when the longest diamine in the series is used. This trend can be explained by considering that the low polarity of HDA contrasts the MW heat transfer, and thus the nanoparticle formation. In routine KT conditions, the high temperature at which the quantification is performed (120 °C) typically allows for almost all amines to react with ninhydrin. However, reactions catalyzed by NCDs are usually conducted at ambient temperature. Consequently, to assess the availability of primary

aliphatic amines to react at ambient temperature, a time-dependent KT at ambient temperature was carried out (Figure 3h,i).[15] In this procedure, the KT at 120 °C is set as the benchmark value and the time-dependent accessibility is expressed as a percentage of this benchmark. In accordance with KT results, accessibility increases from mono- to bi-component synthesis. Interestingly, NCDs-**3** show the highest accessibility value, namely $80\% \pm 5\%$, which is paired with the highest value of KT at 120 °C.

A benchmark amino catalytic transformation was selected to evaluate the activity of NCDs **1**–**4**. Specifically, the investigated reaction is the addition of acetone (**1a**) to *para*-nitro benzaldehyde (**2a**) to give the aldol adduct **3a** (Table 1).[43] All experiments were performed in water, exploiting the generation of nucleophilic enamine intermediates on the surfaces of the nitrogen-doped nanoparticles (catalytic loading: 3% w/V).[27] As expected, no reaction occurred in the absence of the NCDs, thus confirming the catalytic nature of the transformation (Table 1, entry 1). The use of NCDs-**1**, obtained solely from Arg, led to the formation of product **3a** in moderate yield (Table 1, entry 2). Conversely, NCDs-**2** displayed better catalytic performances, providing **3a** in 61% yield (Table 1, entry 3). Interestingly, the yield of the reaction was further enhanced (up to 75%) by using NCDs obtained from BDA, which bears a longer carbon atom chain than EDA (Table 1, entry 4). Lastly, a lower reactivity was observed when NCDs-**4** were used as catalysts (45% yield). Therefore, NCDs-**3** have proven to be the best nano-aminocatalytic systems for the studied reactions. Importantly, these findings are consistent with the total number and accessibility of the surface amino functionalities, both assessed through the KT analysis of the materials (Figure 3). Indeed, NCDs-**3** displayed the highest number of primary amines per gram of material $2100 \pm 550 \, \mu mol \, g^{-1}$. Moreover, the accessibility of the amino groups, which is related to their reactivity towards carbonyl compounds at ambient temperature, was also found to be highest in the case of NCDs-**3** (around 80%). In addition, to evaluate the role played by Arg in the formation of catalytically active NCDs, we synthesized NCDs-**5** starting from a different amino acid, namely L-lysine, and BDA (see Section B.1 of the Supporting Information for details). Interestingly, these nanoparticles yielded product **3a** in a lower chemical yield (66%) than that provided by NCDs-**3** (Table 1, entries 4 and 6). This experi-

Table 1. Catalytic activity of NCDs in the aldol addition reaction between acetone **1a** and *p*-nitrobenzaldehyde **2a**.


Entry	Catalyst	Precursors	Yield 3a [%][a]
1	–	–	0
2	NCDs-**1**	Arg	42 ± 4
3	NCDs-**2**	Arg + EDA	61 ± 5
4	NCDs-**3**	Arg + BDA	75 ± 3
5	NCDs-**4**	Arg + HDA	45 ± 5
6	NCDs-**5**	Lys + BDA	66 ± 5

[a] Yield determined by ^{1}H NMR spectroscopy using 1,1,2-trichloroethene as the internal standard over five independent experiments.

ChemSusChem

Research Article
doi.org/10.1002/cssc.202202399

**Chemistry
Europe**
European Chemical
Societies Publishing

ment demonstrates that the amino acid also has an important role in the production of active NCD-based catalysts. We also compared the catalytic performance of NCDs-**3** with those of simple molecular amines and readily available amine-bearing polymers (see Table 1 of the Supporting Information). Specifically, primary and secondary aliphatic amines, along with aromatic amines, gave negligible results in terms of yield of **3a**. On the other hand, complex commercially available polyamines and polyamides proved themselves to be slightly more active. Nevertheless, NCDs-**3** significantly outperformed all the amines and polyamines tested, hence confirming their superior synthetic potential in the studied transformation (see the Supporting Information, Table S1). To investigate the reaction mechanism, we attempted to detect the formation of aminocatalytic intermediates on the surface of NCDs-**3**. To this end, we exploited ^{19}F NMR spectroscopy. In fact, thanks to its intrinsic high sensitivity, this technique is an attractive tool for the study of superficial changes that occur on carbon dots.[15] Moreover, the detection of ^{19}F nucleus prevents possible overlaps of diagnostic signals with those related to contaminants such as trace solvents, that can usually affect ^{1}H NMR or ^{13}C NMR.[44]

Thus, we chose a series of model primary and secondary amines that are potentially representative of the terminal moieties on the NCDs surface, namely benzylamine, aniline, butylamine and pyrrolidine. These molecular amines were reacted with suitable fluorinated aldehydes – such as 4-fluorobenzaldehyde and 4-fluorophenylacetaldehyde – in DMSO-d_6 to enable the direct detection of the corresponding fluorinated imine and enamine species by ^{19}F NMR analysis.[15] Initially, we employed 4-fluorobenzaldehyde as alpha non-enolizable probe, capable of generating the related molecular imines in situ, that resonate between -108.6 and -110.5 ppm (Figure 4a and Section G.1 of the Supporting Information). Thereafter, under the same reaction conditions, we investigated the formation of superficial fluorinated imines, namely **I**-(NCDs-**3**), on the NCDs-**3** surfaces.
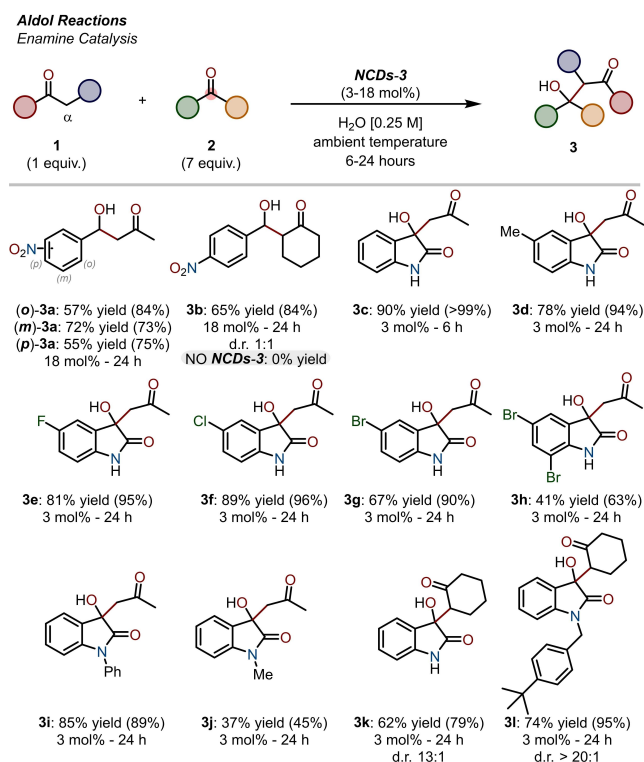
In this case, the appearance of two new broad signals at around -109.4 and -110.6 ppm revealed the formation of various surface imine moieties that experience different chemical environments (Figure 4b). The actual presence of such functional groups was confirmed by comparing the chemical shifts of the previously obtained model imines with those generated on the surface of the carbon nanoparticles. Correspondingly, an α-enolizable fluorinated probe, such as 4-fluorophenylacetaldehyde, was used to produce enamine intermediates through condensation with the corresponding model molecular or superficial amines (Figure 4a and Supporting Information). In this situation, the formation of **II**-(NCDs-**3**) was ascertained by the occurrence of two broad signals between -121 and -122 ppm of the ^{19}F NMR spectrum (Figure 4c). Likewise, closely related signals in terms of chemical shifts were observed by allowing 4-fluorophenylacetaldehyde to react with the abovementioned molecular amines (Figure 4a). Once we had demonstrated that it is possible to easily generate pivotal organocatalytic intermediates on NCDs, we sought to quantify the amount of these surface species on the best catalytically performing materials (NCDs-**3**), therefore tracing back to the original reactive amines present on the nanosized catalysts. By using α,α,α-trifluorotoluene as internal standard for ^{19}F NMR experi-
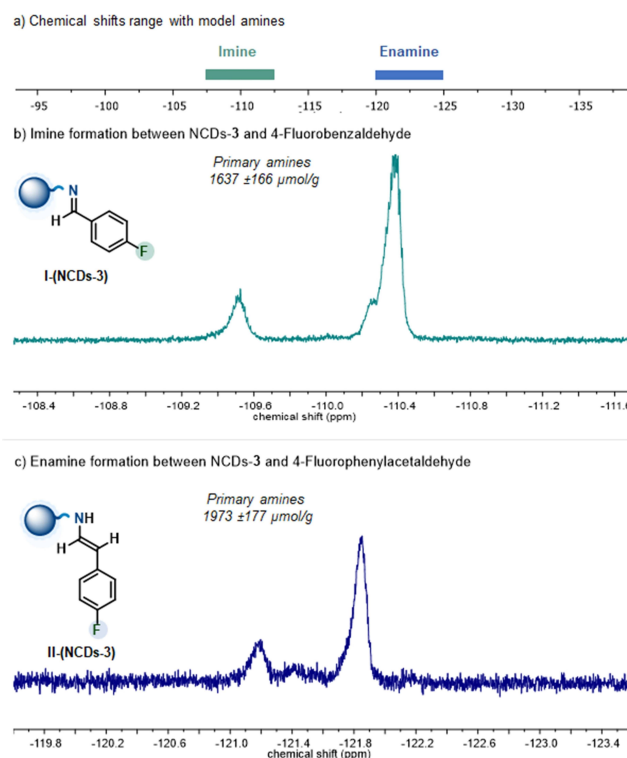
Figure 4. (a) ^{19}F NMR chemical shifts range of imines and enamines formed by mixing the molecular amines and the fluorinated probes. (b) ^{19}F NMR spectrum of NCDs-3 and 4-fluorobenzaldehyde in DMSO-d_6 to detect the superficial imines formation. (c) ^{19}F NMR spectrum of NCDs-3 and 4-fluorophenylacetaldehyde in DMSO-d_6 to detect the superficial enamines formation.

ments, the number of superficial amines on NCDs-**3** turned out to be 1637 ± 166 µmol g^{-1} for the detection though **I**-(NCDs-**3**), whereas it resulted to be 1973 ± 177 µmol g^{-1} when revealed through **II**-(NCDs-**3**) species. These values are very close to those obtained from the KT at 25 °C (1640 ± 550 µmo g^{-1}), hence further demonstrating the reliability of our methodology. With these results in hand, we were able to exploit NCDs-**3** as promising nano-aminocatalytic platforms, that are capable of promoting a wide range of aminocatalytic transformations, ultimately replacing the use of complex molecular catalysts.[13] Building on these premises, NCDs-**3** were employed in a large-scope study to prove the expected generality inferred by their multifunctional surface in a series of aldol additions, Mannich reactions, Knoevenagel condensations, Michael, and tandem Knoevenagel and Michael reactions (Schemes 1–5). We first evaluated the reactivity of different α-enolizable carbonyl compounds **1** and electrophiles **2** to afford the aldol products **3** via enamine-activated aldol reactions. These transformations were conducted in water at ambient temperature (Scheme 1).

In particular, nitro-substituted aldehydes reacted smoothly with acetone and cyclohexanone **2a-b** in the presence of NCDs-**3** (18 mol% of amine that is based on KT analysis at ambient temperature), delivering the corresponding β-hydroxy products **3a–b** in good isolated yields of up to 72%. Interestingly, a very low amount of catalyst (3 mol%) was sufficient to yield products
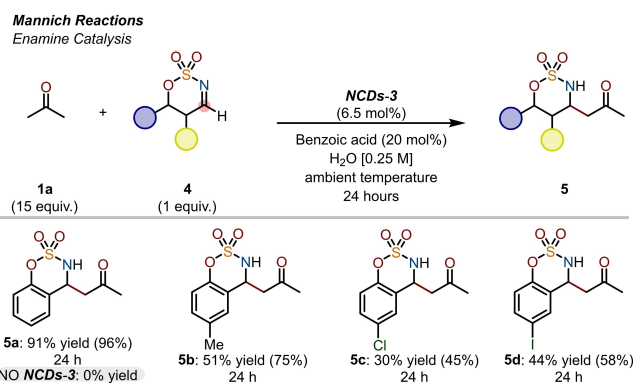
ChemSusChem

Research Article
doi.org/10.1002/cssc.202202399

Chemistry Europe
European Chemical
Societies Publishing

Aldol Reactions
Enamine Catalysis

Scheme 1. Reaction scope study for the aldol additions between α-enolizable carbonyl compounds **1** and electrophiles **2** using NCDs-**3** as nano-organocatalysts. Yields in parentheses were determined by ¹H NMR analyses, using trichloroethylene as an internal standard.

Mannich Reactions
Enamine Catalysis

Scheme 2. Reaction scope study for the Mannich reactions between acetone **1a** and imines **4** using NCDs-**3** as nano-organocatalysts. Yields in parentheses were determined by ¹H NMR analyses, using trichloroethylene as an internal standard.

Knoevenagel Reactions
Iminium Ion Catalysis

Scheme 3. Reaction scope study for the Knoevenagel condensations between malononitrile **6** and electrophiles **2** using NCDs-**3** as nano-organocatalysts. Yields in parentheses were determined by ¹H NMR analyses, using trichloroethylene as an internal standard.

3c–l from good to excellent yields (up to 90%). It is worth noting that when **2b** was employed as reagent, very high *syn* diastereoselectivity was observed (**3k–l**, up to 20:1 diastereomeric ratio) that likely originates in the steric hindrance of the mentioned cyclic ketone.[15] Importantly, no background reactivity in the absence of NCDs-**3** was detected.
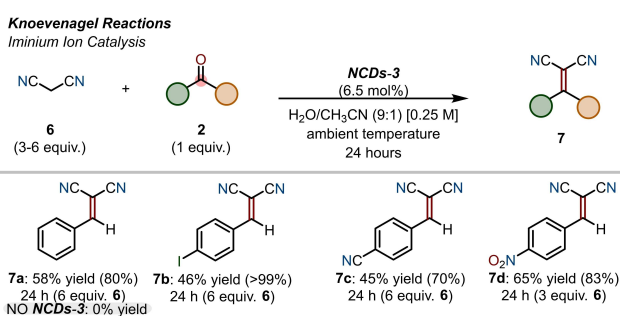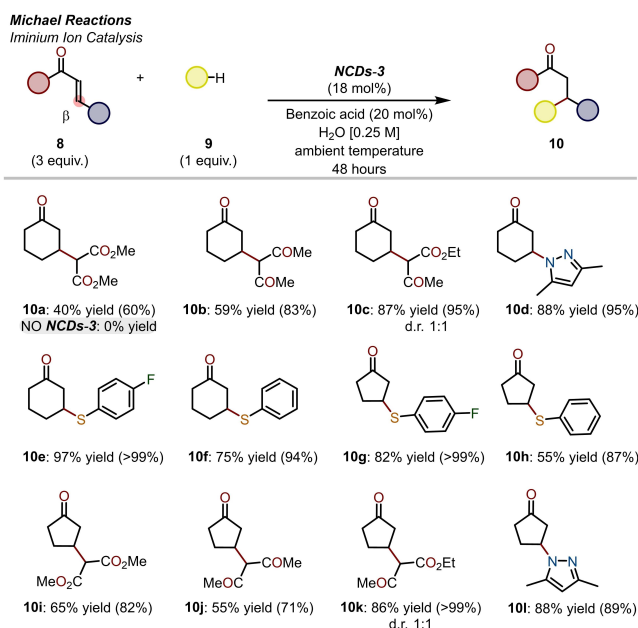
Moreover, we studied the enamine-activated Mannich reaction between acetone **1a** and different imines **4**. The optimized reaction conditions envisioned the use of benzoic acid as additive (20 mol%) and NCDs-**3** as nano-organocatalyst (6.5 mol%) in water at ambient temperature. As shown in Scheme 2, diverse imines **4** bearing alkyl or halogen functionalities on the aromatic ring were suitable substrates, yielding products **5** in moderate to excellent yield (up to 91%). Here too, products **5** were not formed in the absence of NCDs-**3**.

We then turned our attention to the Knoevenagel condensation between malononitrile **6** and electrophiles **2** in water/acetonitrile (9:1) as solvent (Scheme 3).

The formation of unsaturated compounds **7** was driven by the generation of iminium ion intermediates on NCDs-**3** surface (employed at 6.5 mol% loading) through the condensation of aldehydes **2** with the superficial amines, followed by nucleophilic attack of **6**. Control experiments confirmed the pivotal role of NCDs-**3** in the studied transformations. Different electron-withdrawing groups (EWGs) on **2** (–NO₂, –CN, –I) were well tolerated, leading to the formation of products **7** in a very good NMR yield (up to 99%). It is worth mentioning that the

deterioration of the corresponding isolated yields for compounds **7a-d** should be attributed to degradative pathways during their purification (see Supporting Information for details).

Afterwards, we moved to Michael addition of nucleophiles **9** on α,β-unsaturated carbonyl compounds **8** (Scheme 4). These organocatalytic transformations were carried out in aqueous media in the presence of NCDs-**3** (18 mol%) and benzoic acid (20 mol%) over 48 h. Importantly, no reaction took place in the absence of NCDs-**3**. A diverse set of C- and hetero-nucleophiles (e.g., O, N, S) was reacted with cyclohexenone **9a** and cyclopentenone **9b**, hence producing the corresponding adducts **10a–l** in good to excellent isolated yields (up to 97%).

Finally, we exploited the ability of amine-rich NCDs-**3** as multi-functional nano-organocatalysts to carry out tandem Knoevenagel-Michael reactions between 1,3-dicarbonyl compounds **11** and substituted aromatic aldehydes **2** (Scheme 5). These reactions were performed with a particularly low catalyst loading (3.3 mol%) and short reaction times (as low as 1 h) affording the functionalized products **12a–f** in very high yields (up to 98%). In this specific case, a modest background reaction was observed (only a 30% yield of model product **12a**) even though in the standard conditions a 93% yield was obtained.[45]

ChemSusChem

Research Article
doi.org/10.1002/cssc.202202399

**Chemistry
Europe**
European Chemical
Societies Publishing

Scheme 4. Reaction scope study for the Michael additions between α,β-unsaturated carbonyl compounds **8** and nucleophiles **9** using NCDs-**3** as nano-organocatalysts. Yields in parentheses were determined by ^1H NMR analyses, using trichloroethylene as an internal standard.
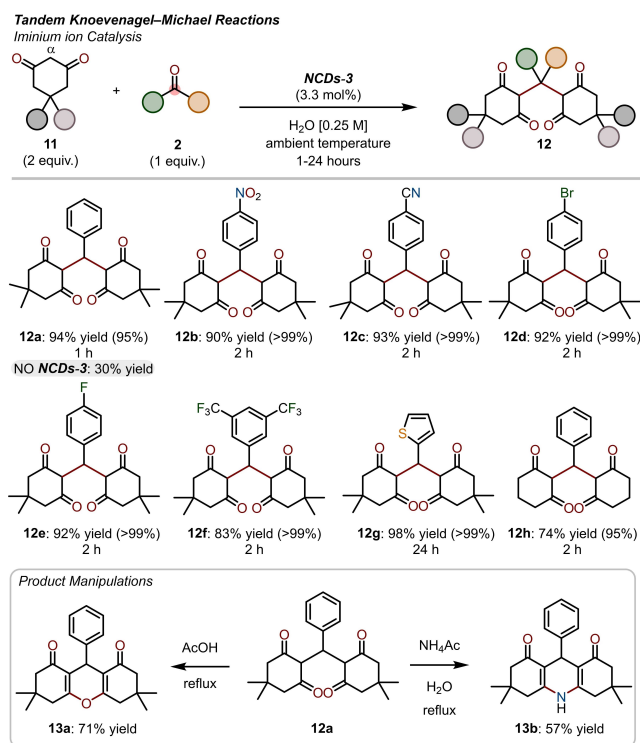
Scheme 5. Reaction scope study for the Tandem Knoevenagel-Michael reactions between 1,3-dicarbonyl compounds **11** and electrophiles **2** using NCDs-**3** as nano-organocatalysts. Yields in parentheses were determined by ^1H NMR analyses, using trichloroethylene as an internal standard.

This transformation turned out to be very general in scope, indeed, different moieties at the *para* position of the aromatic

ring of electrophiles **2** were tolerated, thus providing the corresponding products **12** in excellent yields (up to 98%). Importantly, heteroaromatic aldehydes, such as **2g**, also reacted under the standard conditions to produce **12g** in an almost quantitative yield, although an extended reaction time of 24 h was required. Finally, we demonstrated the synthetic utility of the developed methodology by performing a series of product manipulations on the tandem Knoevenagel-Michael adduct **12a**. In particular, this compound was subjected to further condensation in the presence of an oxygen or nitrogen source to produce xanthenedione **13a** and acridinedione derivatives **13b**, respectively. These two redox-active compounds are of practical importance in the field of organic photocatalysis and biochemistry.[45–48]

Conclusion

Herein, we have presented an in-depth experimental analysis of the aminocatalytic activity for the functionalization of carbonyl compounds by amine-rich carbon dots in relation to their different nanostructure. To do this, we synthetized a new family of NCDs by using L-arginine and different alkyl diamines as starting materials (NCDs **1**–**4**). We subsequently carried out a discrimination of the critical parameters that define the activity of these nanoparticles towards a given organic reaction through a combined set of investigations based on different characterization techniques. In particular, KT analysis, and ^{19}F NMR provided key quantitative insights into the number and the availability of the surface amino groups, which, in turn, depend on the local structure of the nanoparticles' shells. Finally, our proof-of-concept study was condensed into the practical exploitation of the best catalyst (NCDs-**3**) for driving numerous benchmark aminocatalytic transformations. Importantly, these reactions, which proceed through iminium-ion and enamine intermediates, were efficiently catalyzed by NCDs-**3** in water solution. To conclude, we believe that this work has the potential to inspire future rational design of NCD-based amino-catalysts for other organic reactions.

Experimental Section

General procedures for the synthesis of NCDs **1**–**5** (see the Supporting Information for details). Mono-component synthesis: Arg (87.0 mg, 0.5 mmol, 1 equiv.) and Milli-Q water (100.0 μL) were added into a sealable microwave reaction vessel and subsequently heated in a microwave reactor (200 W) at 240 °C, 26 bar for 180 s. Bi-component synthesis: Arg (87.0 mg, 0.5 mmol, 1 equiv.) or Lys (73.1 mg, 0.5 mmol, 1 equiv.), Milli-Q water (100.0 μL), along with one of the alkyl diamines selected for this experimental work (Figure S1), namely EDA or BDA or HDA (0.5 mmol, 1 equiv.) were added into a sealable microwave reaction vessel and subsequently heated in a microwave reactor (200 W) at 240 °C for 180 s. The solution of the starting materials changes color from transparent to brown because of the formation of CDs. The solution was then diluted with water and filtered through a 0.1 μm PTFE microporous membrane. The crude so obtained was dialyzed against Milli-Q water through a dialysis membrane (0.5–1 kDa cut-off) Float-A-Lyzer® for 48 h. The resulting aqueous solution of CDs was

lyophilized resulting in an orange-to-yellow fluffy solid. The solid was collected and its weight was measured. To prevent the absorption of moisture, the samples have been kept in a desiccator.

Conflict of Interest

The authors declare no conflict of interest.

Data Availability Statement

The data that support the findings of this study are available in the supplementary material of this article.

[1] F. Arcudi, L. Đorđević, M. Prato, *Acc. Chem. Res.* **2019**, *52*, 2070–2079.
[2] V. Corti, B. Bartolomei, M. Mamone, G. Gentile, M. Prato, G. Filippini, *Eur. J. Org. Chem.* **2022**, e202200879.
[3] L. Đorđević, F. Arcudi, M. Cacioppo, M. Prato, *Nat. Nanotechnol.* **2022**, *17*, 112–130.
[4] J. Liu, R. Li, B. Yang, *ACS Cent. Sci.* **2020**, *6*, 2179–2195.
[5] R. de Boëver, J. R. Town, X. Li, J. P. Claverie, *Chem. Eur. J.* **2022**, *28*, e202200748.
[6] S. Y. Lim, W. Shen, Z. Gao, *Chem. Soc. Rev.* **2014**, *44*, 362–381.
[7] C. Xia, S. Zhu, T. Feng, M. Yang, B. Yang, *Adv. Sci.* **2019**, *6*, 1901316.
[8] L. Đorđević, F. Arcudi, M. Prato, *Nat. Protoc.* **2019**, *14*, 2931–2953.
[9] A. Döring, E. Ushakova, A. L. Rogach, *Light-Sci. Appl.* **2022**, *11*, 75.
[10] B. Bartolomei, J. Dosso, M. Prato, *Trends Chem.* **2021**, *3*, 943–953.
[11] R. Manjupriya, S. M. Roopan, *J. Mater. Sci.* **2021**, *56*, 17369–17410.
[12] G. A. M. Hutton, B. C. M. Martindale, E. Reisner, *Chem. Soc. Rev.* **2017**, *46*, 6111–6123.
[13] C. Rosso, G. Filippini, M. Prato, *ACS Catal.* **2020**, *10*, 8090–8105.
[14] Z. Zhao, S. Reischauer, B. Pieber, M. Delbianco, *Green Chem.* **2021**, *23*, 4524–4530.
[15] G. Filippini, F. Amato, C. Rosso, G. Ragazzon, A. Vega-Peñaloza, X. Companyó, L. Dell'Amico, M. Bonchio, M. Prato, *Chem* **2020**, *6*, 3022–3037.
[16] F. Yan, Y. Jiang, X. Sun, Z. Bai, Y. Zhang, X. Zhou, *Microchim. Acta* **2018**, *185*, 424.
[17] Z. Kang, S. T. Lee, *Nanoscale* **2019**, *11*, 19214–19224.
[18] C. Rosso, G. Filippini, M. Prato, *Chem. Eur. J.* **2019**, *25*, 16032–16036.
[19] Z. Zhao, B. Pieber, M. Delbianco, *ACS Catal.* **2022**, *12*, 13831–13837.
[20] M. Hasani, H. R. Kalhor, *ACS Catal.* **2021**, *11*, 10778–10788.
[21] S. Liu, Y. He, Y. Liu, S. Wang, Y. Jian, B. Li, C. Xu, *Chem. Commun.* **2021**, *57*, 3680–3683.
[22] A. Dondoni, A. Massi, *Angew. Chem. Int. Ed.* **2008**, *47*, 4638–4660; *Angew. Chem.* **2008**, *120*, 4716–4739.
[23] X. Pei, D. Xiong, H. Wang, S. Gao, X. Zhang, S. Zhang, J. Wang, *Angew. Chem. Int. Ed.* **2018**, *57*, 3687–3691; *Angew. Chem.* **2018**, *130*, 3749–3753.
[24] M. O. Simon, C. J. Li, *Chem. Soc. Rev.* **2012**, *41*, 1415–1427.
[25] A. Chanda, V. v. Fokin, *Chem. Rev.* **2009**, *109*, 725–748.
[26] U. M. Lindström, *Chem. Rev.* **2002**, *102*, 2751–2772.
[27] M. P. van der Helm, B. Klemm, R. Eelkema, *Nat. Chem. Rev.* **2019**, *3*, 491–508.
[28] T. Kitanosono, K. Masuda, P. Xu, S. Kobayashi, *Chem. Rev.* **2018**, *118*, 679–746.
[29] F. Arcudi, L. Đorđević, M. Prato, *Angew. Chem. Int. Ed.* **2016**, *55*, 2107–2112; *Angew. Chem.* **2016**, *128*, 2147–2152.
[30] F. Rigodanza, M. Burian, F. Arcudi, L. Đorđević, H. Amenitsch, M. Prato, *Nat. Commun.* **2021**, *12*, 2640.
[31] M. B. Gawande, S. N. Shelke, R. Zboril, R. S. Varma, *Acc. Chem. Res.* **2014**, *47*, 1338–1348.
[32] Y. Ji, X. Yang, Z. Ji, L. Zhu, N. Ma, D. Chen, X. Jia, J. Tang, Y. Cao, *ACS Omega* **2020**, *5*, 8572–8578.
[33] P. K. Smith, R. I. Krohn, G. T. Hermanson, A. K. Mallia, F. H. Gartner, M. D. Provenzano, E. K. Fujimoto, N. M. Goeke, B. J. Olson, D. C. Klenk, *Anal. Biochem.* **1985**, *150*, 76–85.
[34] H. D. Hill, J. G. Straka, *Anal. Biochem.* **1988**, *170*, 203–208.
[35] B. Bartolomei, A. Bogo, F. Amato, G. Ragazzon, M. Prato, *Angew. Chem. Int. Ed.* **2022**, *61*, e202200038.
[36] Y. Wang, S. Kalytchuk, Y. Zhang, H. Shi, S. v. Kershaw, A. L. Rogach, *J. Phys. Chem. Lett.* **2014**, *5*, 1412–1420.
[37] J. A. Boiani, *J. Chem. Educ.* **1986**, *63*, 724.
[38] J. B. Essner, J. A. Kist, L. Polo-Parada, G. A. Baker, *Chem. Mater.* **2018**, *30*, 1878–1887.
[39] Y. Xiong, J. Schneider, E. v. Ushakova, A. L. Rogach, *Nano Today* **2018**, *23*, 124–139.
[40] G. Candiano, M. Bruschi, L. Musante, L. Santucci, G. M. Ghiggeri, B. Carnemolla, P. Orecchia, L. Zardi, P. G. Righetti, *Electrophoresis* **2004**, *25*, 1327–1333.
[41] E. Kaiser, R. L. Colescott, C. D. Bossinger, P. I. Cook, *Anal. Biochem.* **1970**, *34*, 595–598.
[42] M. Garrido, L. Gualandi, S. di Noja, G. Filippini, S. Bosi, M. Prato, *Chem. Commun.* **2020**, *56*, 12698–12716.
[43] B. List, R. a. Lerner, C. F. Barbas III, *J. Am. Chem. Soc.* **2000**, *122*, 2395–2396.
[44] E. N. G. Marsh, Y. Suzuki, *ACS Chem. Biol.* **2014**, *9*, 1242–1250.
[45] J. J. Yu, L. M. Wang, J. Q. Liu, F. lou Guo, Y. Liu, N. Jiao, *Green Chem.* **2010**, *12*, 216–219.
[46] S. Khandelwal, Y. K. Tailor, M. Kumar, *J. Mol. Liq.* **2016**, *215*, 345–386.
[47] R. Singla, K. B. Gupta, S. Upadhyay, M. Dhiman, V. Jaitak, *Bioorg. Med. Chem.* **2018**, *26*, 266–277.
[48] H.-J. Timpe, S. Ulrich, C. Decker, J. P. Fouassier, *Macromolecules* **1993**, *26*, 4560–4566.